Proceedings of the Global Congress on ICM: Lessons Learned to Address New Challenges
30 Oct - 3 Nov 2013, Marmaris, Turkey, E. Özhan (Editor), pp. 665-676

Submesoscale Eddies Seen by Spaceborne Radar

Svetlana Karimova[(1)] and Martin Gade[(2)]

[(1)] Space Research Institute of RAS, 117997 Moscow, Russia
Tel: +7-495-333 42 56 Fax: +7-495-333 10 56
E-mail: feba@list.ru
[(2)] Universität Hamburg, D-20146 Hamburg, Germany
Tel: +49 40 42838 5450 Fax: +49 40 42838 7471,
Email: martin.gade@uni-hamburg.de

Abstract

In the present study, synthetic aperture radar (SAR) imagery was used to derive statistics on spiral eddies in the eastern Mediterranean and Black seas. The dataset used consists of about 1700 medium resolution Envisat ASAR and ERS-2 SAR images obtained in 2009-2011. A comprehensive analysis of the eddy occurrence in SAR imagery was performed, thus providing insight into the eddies' spatial and temporal distribution and the eddy 'density', i.e. the number of eddies per square unit. The analyses of the temporal variability of the derived above-mentioned statistical parameters revealed their strong seasonality, whose main reasons were suggested to be the seasonal variability of the encountered wind speed and surfactant films presenting.

Introduction

It is well known that mesoscale eddies are essential in forming hydrological and biological structures of seawater. At first, they greatly participate in the cross-shelf water transport and thus contribute to water mixing and self-cleaning processes. At second, eddies affect phytoplankton productivity in marine ecosystems. Spiral, or submesoscale, eddies with a diameter less than the baroclinic Rossby radius of deformation (about 12-20 km for the eastern Mediterranean and Black seas) are also considered to play a significant role in this respect, though this still needs to be clarified (Lapeyre and Klein, 2006).

Despite the fact that spiral eddies on the sea surface were first seen from space more than 40 years ago, there is still a lot of uncertainties concerning their origin, distribution, and lifetime. Nowadays many efforts are being undertaken in order to study this type of ocean stirring through laboratory (Voropayev and Afanasyev, 1992; Boubnov and Golitsyn, 1995; Golitsyn, 2012) and numerical (Eldevik and Dysthe, 2002; Shen and Evans, 2002; Akitomo, 2010; Callendar et al., 2011) modeling as well as satellite (Dokken and Wahl, 1996; Munk et al., 2000; DiGiacomo and Holt, 2001; Karimova, 2012; Alpers et al., 2013), high frequency radar (Bassin et al., 2005), and in situ (Marmorino et al., 2010) observations.

Due to their high spatial resolution, wide swath of observation, and independence on cloud cover and sunlight conditions, satellite-borne synthetic aperture radar (SAR) sensors are an effective tool to gain more information on spiral eddies, particularly in coastal waters. In the present study, SAR imagery was used to derive statistics on spiral eddies in the eastern Mediterranean and Black seas.

Regions of Interest

The Mediterranean Sea

The Mediterranean Sea extends for about 3860 km in the east-west direction, so it combines a variety of physical and bio-geochemical conditions. The sea consists of a series of deep depressions connected to each other. The eastern part of the sea regarded in the present paper includes the Ionian, Adriatic, and Aegean Seas as well as Levantine Basin.

General surface circulation of the Mediterranean Sea is described to have quasi-permanent counterclockwise circuits, in both the western and eastern basins. Physical Oceanography of the Eastern Mediterranean (POEM) experiment represented the Atlantic Water (AW) path as an offshore jet (so called Mid-Mediterrenean Jet) crossing the basin in its central part with mesoscale eddies forming on both sides (Robinson et al., 1991). Satellite infrared imagery was used for studying general and mesoscale circulation of the Mediterranean Sea by Taupier-Letage (2008). The thermal signature of AW was tracked along the southern continental slopes of both basins. This flow meanders and generate anticyclonic eddies that have lifetimes of several months. This intense mesoscale activity shows a very high variability in both space and time. Such mesoscale eddies were shown to play a significant role in transporting AW from the periphery toward the central part of the basin.

The Black Sea

In spite of relatively simple geometry of the basin and its bottom topography the Black Sea surface circulation has a very complicated spatial structure and is characterized by strong seasonal, synoptic, and interannual variabilities. Its most prominent feature is a basin-scale boundary current cyclonically flowing along the continental slope, namely the Rim Current. This flow is supposed to originate from (i) wind forcing peculiarities (i.e. cyclonic wind vorticity over the basin) and (ii) freshened water area along the seashore due to river runoff enhancing the Ekman circulation going in cyclonic direction (Zatsepin et al., 2003).

The Black Sea has a very peculiar pattern of mesoscale eddy formation. One of the characteristic features of the basin is so called Black Sea quasi-permanent anticyclonic eddies that originated from the combined effect of hydrodynamic instability of the Rim Current and basin configuration. The Sevastopol, Batumi, and Caucasus eddies are traditionally regarded as the greatest and most stable of the Black Sea quasi-permanent eddies (Oguz et al., 1992).

Another typical Black Sea circulation element is near-shore anticyclonic eddies forming within a zone of coastal anticyclonic current vorticity between the coast and the midstream of the Rim Current. They stretch along the coast due to lateral friction, so their most prominent feature is an elongated shape (Titov and Savin, 2008).

There is also a number of non-stationary mesoscale eddies in the Black Sea discovered due to satellite visible and infrared imagery (Karimova, 2011). The most important of them are as follow: (i) eddy dipoles (mushroom-like currents), (ii) eddy chains, and (ii) eddies of the Anatolian coast. The area of the most frequent observation of eddy chains, both anticyclonic and cyclonic, is one to the south from the Kerch Strait. Mushroom-like currents were mostly detected in the Rim Current zone along the western and eastern sea coasts.

Data and Methods

The present study is based on an analysis of 1416 Envisat Advanced SAR (ASAR) Wide Swath (WS) and 256 ERS-2 SAR medium resolution imagery acquired over the Black Sea and eastern Mediterranean Basin during the whole years 2009 thru 2011. The spatial resolution of the ASAR WS imagery is about 150 m. Fig. 1 shows the areal coverage of the region of interest with ASAR images for the whole observation period.

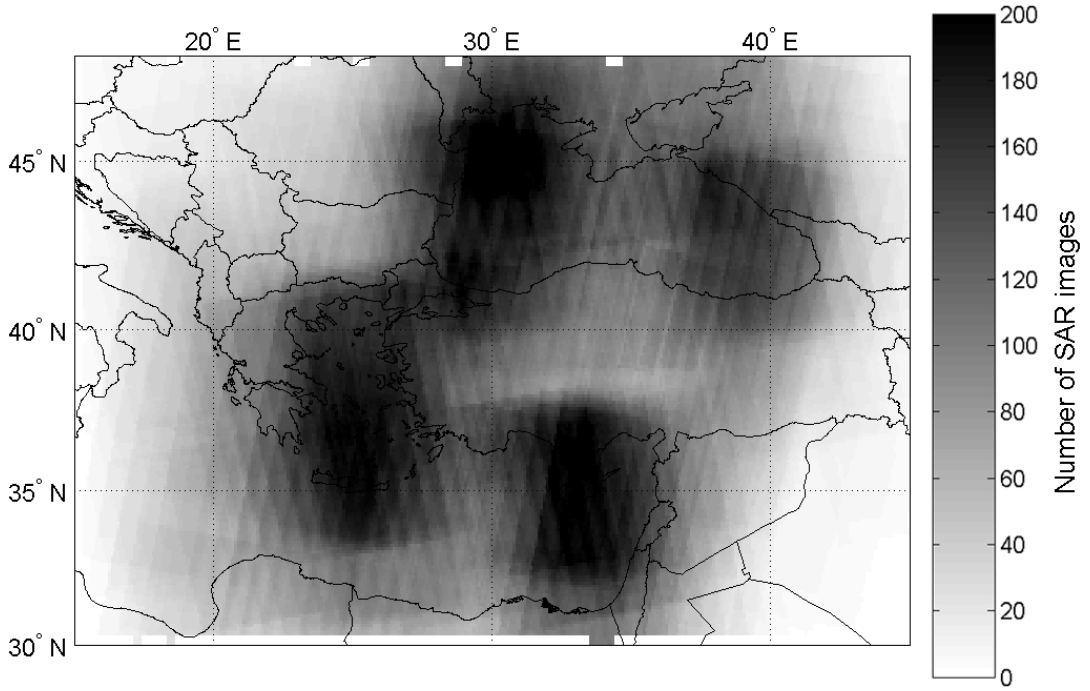

Fig. 1: SAR image coverage of the Black and Eastern Mediterranean seas in 2009-2011.

For some parts of the region of interest (the Aegean Sea, western part of the Black Sea, and eastern-most Mediterranean Sea), more than 200 ASAR scenes are available per unit area, whereas others areas were imaged less than 40 times in 2009-2011.

In general, submesoscale eddies manifest in SAR imagery due to two main mechanisms, namely the accumulation of surfactants and wave/current interactions (Karimova, 2012). At low to moderate wind speeds (of 3-5 m/s) the former is the main mechanism and eddies usually appear in SAR images due to the presence of natural films on the sea surface (Espedal et al., 1998). Surfactants dampen small-scale surface waves, thereby reducing the radar backscattering from the sea surface (Alpers and Hühnerfuss, 1989), and if they accumulate along the shear lines, which are associated with the spiral flow, the eddies become visible on SAR imagery (Gade et al., 2013). Since this effect causes the eddies to be marked dark, for shortness sake, eddies visualized due to slicks are hereinafter referred to as "black" eddies. In Fig. 2a, an example of "black" eddies manifestation in SAR imagery is presented. This image of size 80 km × 50 km was acquired on 03.09.2009 and shows the northern part of the Ionian Sea. In the bottom of the image, the surface films mark a strong flow representing the northern part of an anti-cyclonic eddy. On the periphery of the eddy, a chain of (cyclonic) "black" eddies can be inferred, which are likely to result from the interaction of the general flow within the eddy with the adjacent waters.

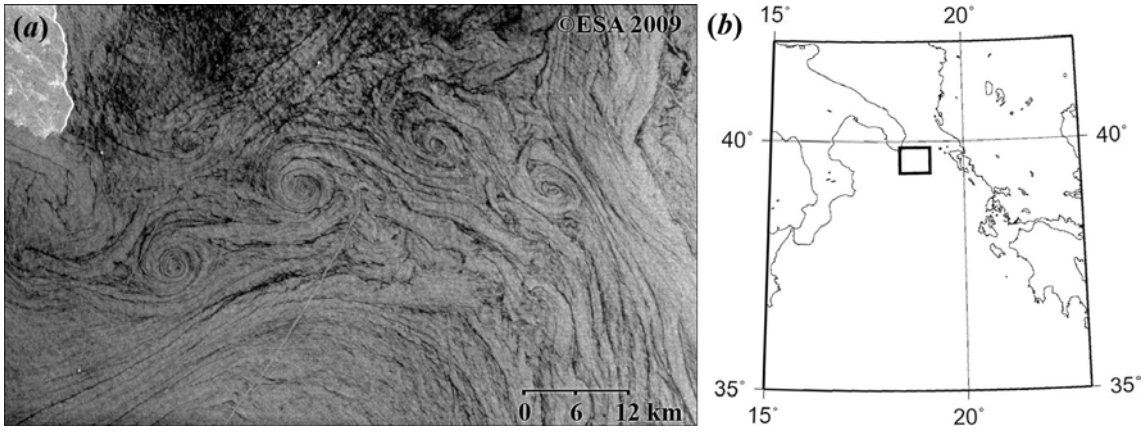

Fig. 02: Group of "black" eddies in ERS-2 SAR image obtained on 03.09.2009 at 09:24 UTC (a) and location of the image on a map of the Mediterranean Sea (b).

At wind speeds of 5-7 m/s, surfactant films start to disrupt, and as a result those dark spiral lines representing "black" eddies disappear (Dokken and Wahl, 1996). At higher wind speeds eddies appear in SAR imagery only as a result of wave/current interactions along the lines of current shear, which manifest as bright curved lines. Dokken and Wahl (1996) reported that due to this mechanism eddies can be visualized in SAR imagery at wind speeds as high as 12 m/s. Since the radar backscattering is locally enhanced due to this effect, eddies of this type are hereinafter referred to as "white" eddies. An example of such eddy manifestations is provided in Fig. 3a. This ERS-2 SAR image (52 km x 44 km) was acquired on 23.10.2010 to the west from the Menorca Island. A spiral "white" eddy (marked with a bigger arrow) can be inferred from a bright spiral signature in the centre of the image. Another smaller eddy can be seen in the upper left corner of the image (marked with a smaller arrow).

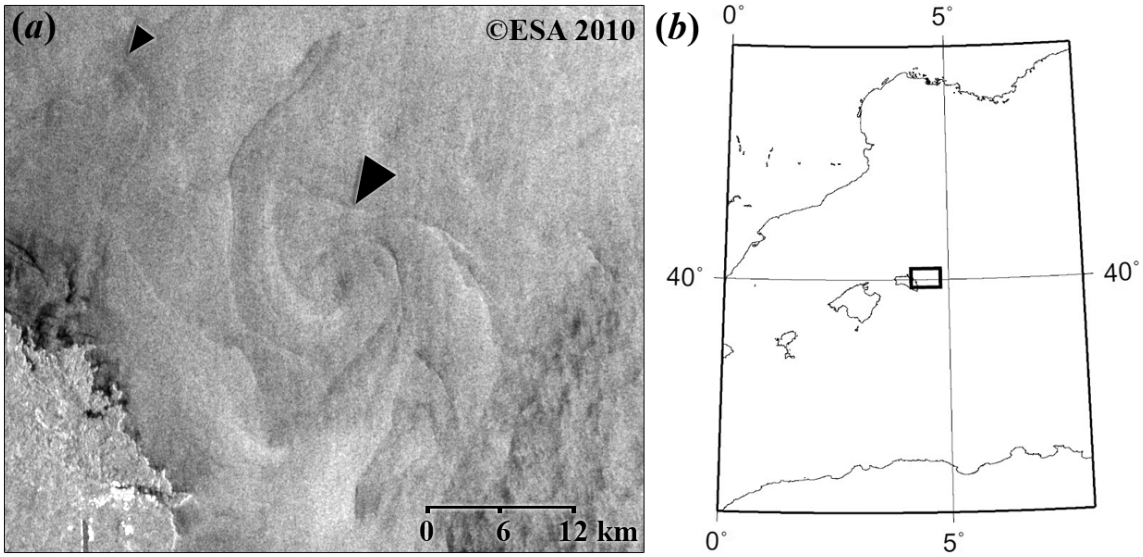

Fig. 03: "White" eddies manifestation in ERS-2 SAR image obtained on 23.10.2010 at 10:21 UTC (a) and location of the image on a map of the Mediterranean Sea (b).

All SAR images used for the present investigation were visually inspected and for each detected eddy, its centre coordinates were recorded. The results of our statistical analysis of submesoscale eddies (with diameters less than approx. 20 km) are provided in the following section.

Results of the Observations

In total, 765 ASAR images contained some eddy manifestations out of 1672 images analyzed, i.e. eddies were found in 46% of images. In this imagery, totally 12.942 submesoscale eddies were detected. Most frequently eddies could be seen during autumn when about 34% of eddies were found. About 63% of eddies were visible due to surfactant films and the rest 37%, due to wave/current interactions.

The majority (about 90%) of the eddies found were cyclonical (counter-clockwise). In the Aegean Sea, share of anti-cyclonic eddies was a bit higher than in average. Apparently it is due to the presence of multiple islands in this basin which cause lateral friction and consequently more frequent generation of anti-cyclonic eddies.

The distribution of the eddies detected among two basins (the Black and eastern Mediterranean seas) and eddy manifestation types ("black" and "white") is shown in Table 1.

Table 1: Distribution of the eddies detected among the basins and eddy manifestation types.

Basin	**"Black" eddies**	**"White eddies"**	**Total**
Black Sea	5230	2607	7837
Eastern Mediterranean	2987	2118	5105
Total	8217	4725	12.942

As it can be seen from the Table 1, in the Black Sea there were more "black" eddies discovered than in the eastern Mediterranean basin. Probably it is accounted for by the less bioproductivity of the Mediterranean waters and consequent lack of surfactant films to visualize "black" eddies. At the same time, numbers of "white" eddies for the two basins were quite close that witnesses about similar hydrodynamic and wind conditions within them.

Figs. 4a and b show the spatial distribution of the detected "black" and "white" eddies, respectively, for the entire period 2009-2011.

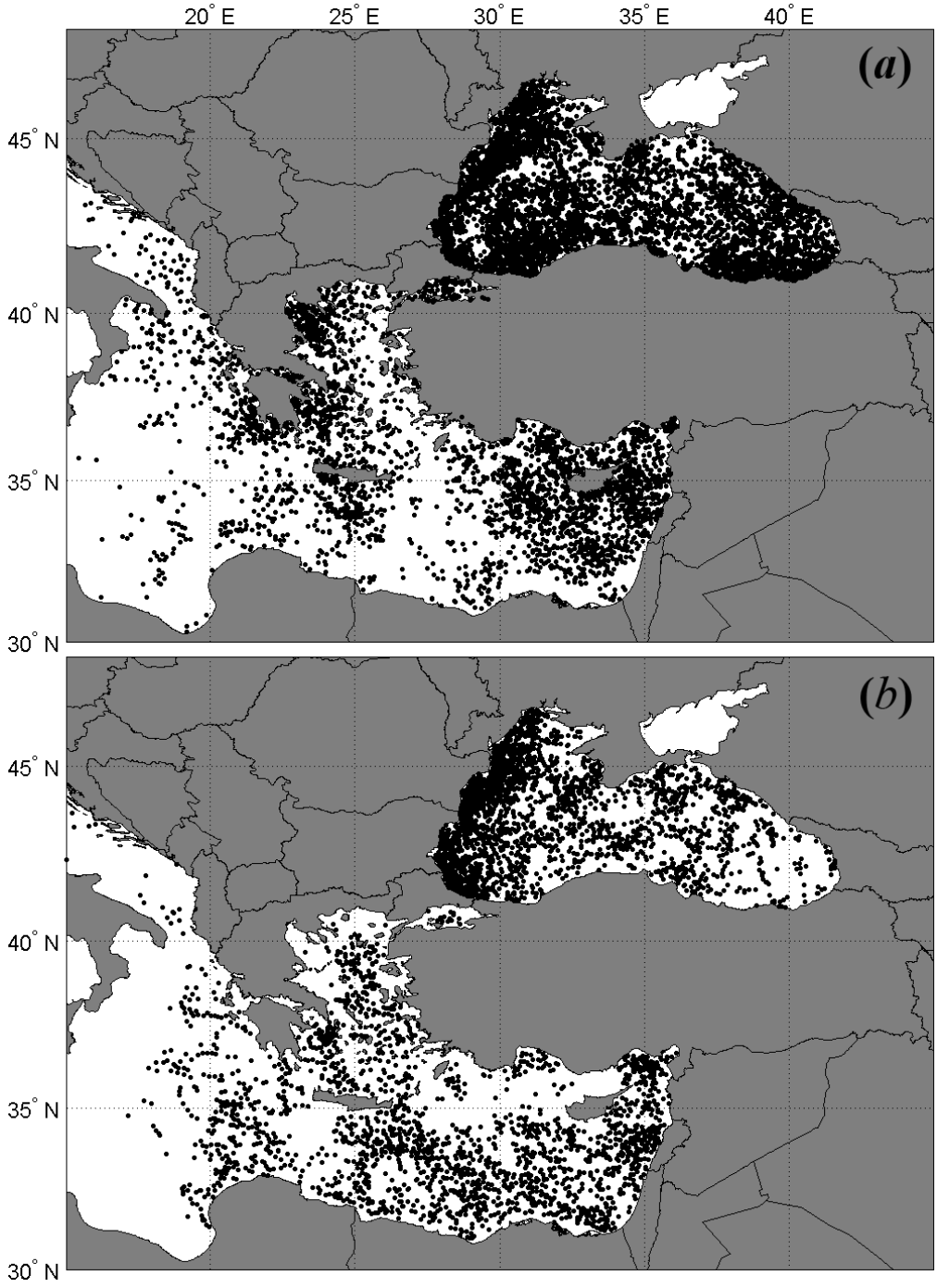

Fig. 4: Spatial distribution of "black" (a) and "white" (b) submesoscale eddies.

"Black" eddies in the Black Sea were found almost all over the basin (Fig. 4a). In the eastern Mediterranean, they were frequently detected (i) in the areas with maximum coverage density (Fig. 1) and (ii) in the near-coastal areas. The former may be an indicator of homogeneous, in general, spatial distribution of "black" eddies generation, while the latter seems to be quite natural. Indeed, since lower wind speeds are needed for the visualization of "black" eddies, more of them should be found in coastal zones, where the interaction with, and the sheltering by, the land reduces the mean wind speed. Moreover, in addition to the constraints given by the SAR imaging of surface films, both the shallow bathymetry in coastal zones and the closer distance to the shore should have an impact on the generation of eddies.

"White" eddies were mostly concentrated along the western coast of the Black Sea which can be explained by high wind and drift current speeds prevailing in this area. Additionally, "white" eddies were frequently detected in the offshore regions of the Black and Mediterranean seas (Fig. 4b). Again, the overall higher (mean) wind speed on the open sea supports the generation/visualization of "white" eddies, but also reduces the visibility of surfactants on SAR imagery.

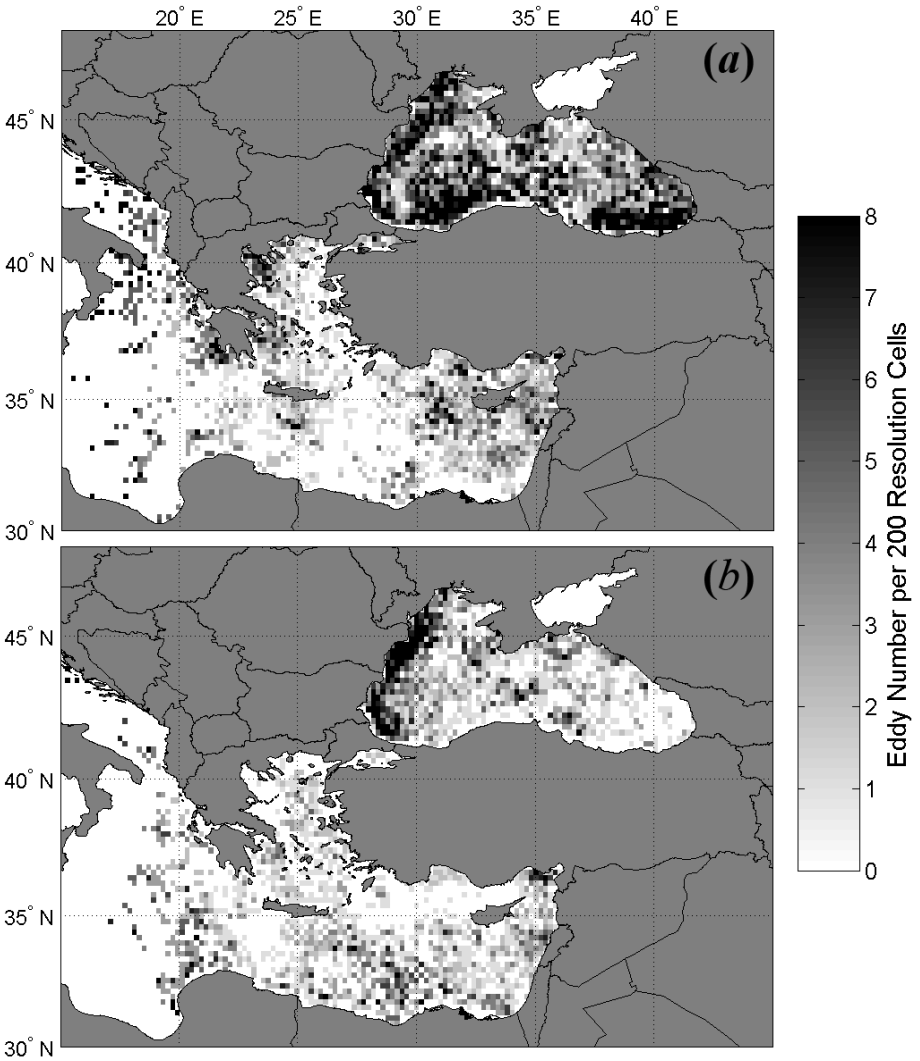

Fig. 05: Normalized eddy density (i.e. the number of eddies per image) of "black" (a) and "white" (b) eddies.

Since "white" eddies were found also in the areas with low image density, it is unlikely that the heterogeneous distribution of the "white" eddies (and of the "black" eddies as well) is just a manifestation of the heterogeneous coverage of the total area by SAR imagery. Instead, hydrodynamic differences, in combination with a different bathymetry and wind climatology in either parts of the basin, must be responsible for the observed differences in eddy density. In order to support this statement, we have calculated normalized densities, i.e. the number of (detected) eddies per image and per resolution cell (of size 0.2°×0.2°), for convenience multiplied by 200. The respective maps are shown in Fig. 5 and demonstrate that the general distribution of both "black" and "white" eddies is looking the same, with or without normalization.

The seasonal variability of eddy distribution is depicted in Figs. 6 and 7. In this analysis, January, February, and March were regarded as winter, April, May, and June, as spring, July, August, and September, as summer, and October, November, and December, as autumn.

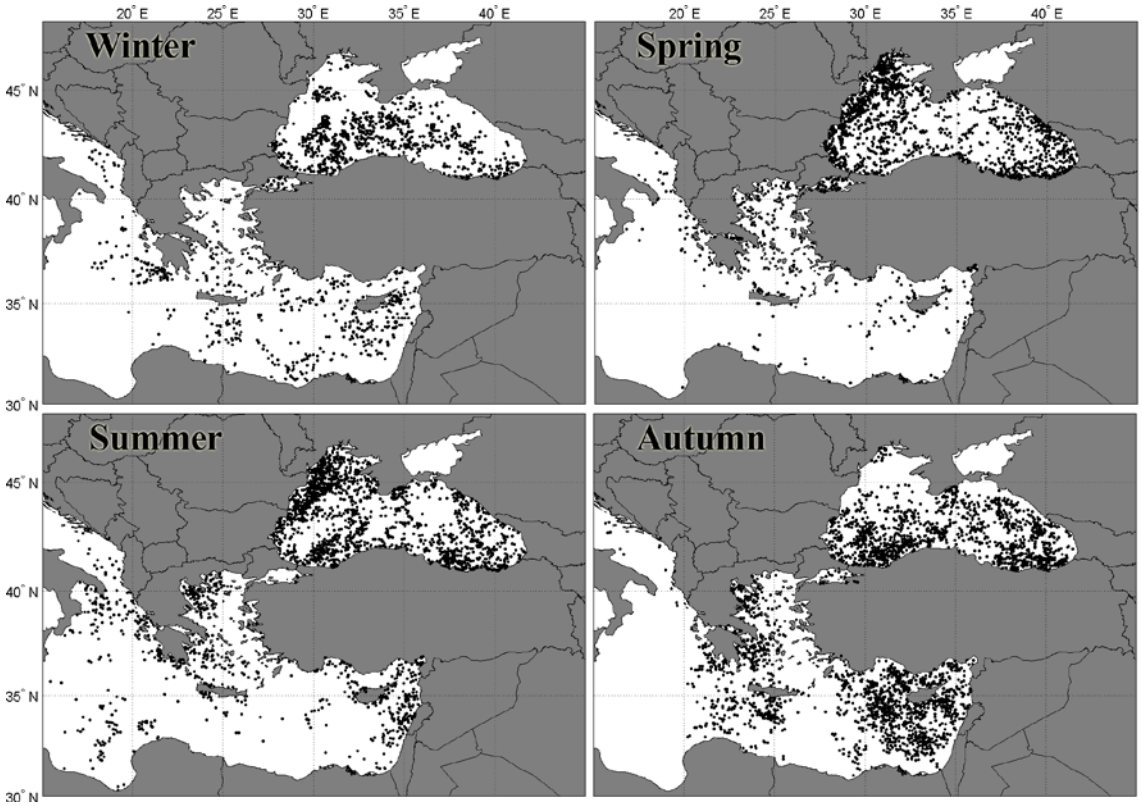

Fig. 06: Spatial distribution of "black" eddies at different seasons.

On analysis of the Fig. 6 we can notice that during the warm period (i.e. spring and summer) "black" eddies were encountered mostly in the near-coastal zone and especially in the north-western part of the Black Sea, which can be explained (i) by arriving a great amount of surfactants with river runoff and (ii) by higher bioproductivity of phytoplankton in those regions that also provides additional surface films. It is noteworthy that in the Mediterranean Sea most of the "black" eddies were found during autumn. Apparently during this time (i) there are enough surfactant films accumulated during summer and (ii) upper mixed layer depth is still reduced after summer heating that can cause greater submesoscale eddy activity.

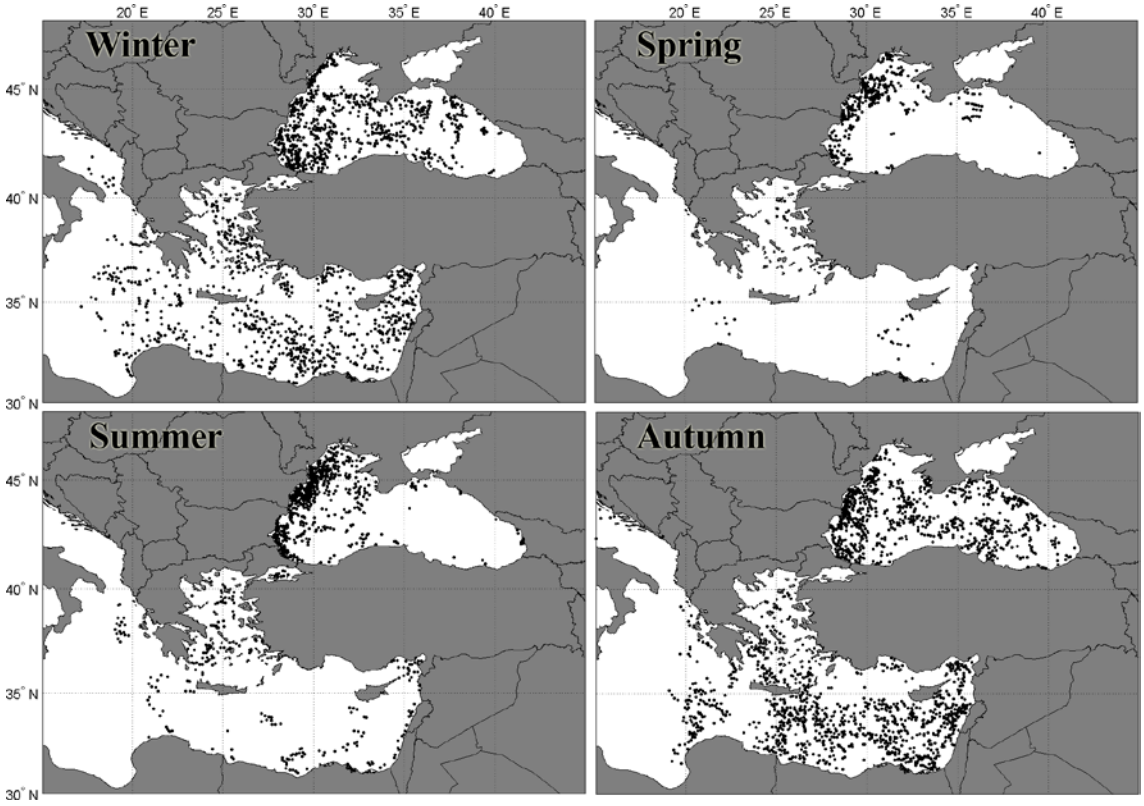

Fig. 07: Spatial distribution of "white" eddies at different seasons.

"White" eddies were discovered mostly during cold season (Fig. 7) that is apparently caused by higher wind speeds needed for "white" eddy visualization. During the warm period "white" eddies were detected in the western-most part of the Black Sea, where wind and current speeds are high enough to visualize "white" eddies. Again, most of "white" eddies in the Mediterranean Sea were found during autumn.

Conclusions

We used about 1700 Envisat ASAR WS and ERS-2 SAR medium resolution images acquired in 2009-2011 over the Black and eastern Mediterranean seas to reveal the spatial and temporal (seasonal) distribution of submesoscale eddies and thus investigate submesoscale eddy activity in these basins and eddy visibility in SAR imagery.

In total, about 13.000 submesoscale eddies were found. Eddies were detected in about 46% of the images analyzed. Most of the eddies were cyclonic (about 90%) though in the Aegean Sea the percentage of anti-cyclonic eddies was higher due to local coastal topography. About 63% of eddies manifested in the SAR imagery due to surfactant films, i.e. they were "black" eddies, while the rest 37%, through wave-current interactions ("white" eddies). Most of the "black" eddies (about 64%) were detected in the Black Sea presumably due to higher bioproductivity and resulting higher concentration of surfactants there. "White" eddies were distributed more or less evenly between the two basins thus letting us conclude about close wind conditions above them, which cause similar effects on surface currents.

Most of the images analyzed covered the western part of the Black Sea, eastern edge of the Mediterranean Sea as well as the Aegean Sea and therefore most of the eddies detected were also located there. However, the normalized densities (number of eddies per image within a resolution cell) show evidence that the observed heterogeneity is not simply due to the inhomogeneous coverage by SAR imagery, especially for "white" eddies.

"Black" eddies were found mostly in coastal areas where there are more favourable conditions for eddy generation (e.g., via later friction) and visualization (due to higher concentration of surfactants). "White" eddies were found both in the coastal area and further offshore where both wind and surface currents can reach higher speeds. Area with especially frequent observation of "white" eddies was one along the western coast of the Black Sea. In the Mediterranean Sea such an area was the southern part of the Levantine Basin.

Due to seasonal variability of the near-surface wind speed and availability of the surfactant films "black" eddies were observed mostly during the warm period (spring and summer), while "white" ones, during the cold period (autumn and winter). In the area along the western coast of the Black Sea, where winds and resulting currents are strong enough throughout the year, "white" eddies were found during all the seasons. In the Mediterranean Sea, eddies of both types of visualization were mostly detected during autumn when there are apparently favourable conditions for eddy generation (due to thin upper mixed layer) and visualization (due to available surfactants and required near-surface wind speeds).

Acknowledgements

This work was supported within the framework of the Federal Target Program "Scientific and scientific-pedagogical personnel of innovative Russia" in 2009-2013. SAR data were obtained under the grant of the European Space Agency # 14120 "Spiral eddy statistical analyses for the Mediterranean Sea using Envisat ASAR Imagery (SESAMeSEA)".

References

Alpers, W., Brandt, P., Lazar, A., Dagorne, D., Sow, B., Faye, S., Hansen, M., Rubino, A., Poulain, P.M. and Brehmer, P. (2013), "A small-scale oceanic eddy off the coast of West Africa studied by multi-sensor satellite and surface drifter data", *Remote Sens. Environ.*, 129: 132-143.

Alpers, W. and Hühnerfuss, H. (1989), "The damping of ocean waves by surface films: A new look at an old problem", *J. Geophys. Res.*, 94 (C5), 6251–6265.

Bassin, C.J., Washburn, L., Brzezinski, M. and McPhee-Shaw, E. (2005), "Sub-mesoscale coastal eddies observed by high frequency radar: A new mechanism for delivering nutrients to kelp forests in the Southern California Bight", *Geophys. Res. Lett.*, 32, L12604, doi:10.1029/2005GL023017.

Bidigare, R.R., Benitez-Nelson, C., Leonard, C.L., Quay, P.D., Parsons, M.L., Foley, D.G. and Seki, M.P. (2003), "Influence of a cyclonic eddy on microheterotroph biomass and carbon export in the lee of Hawaii", *Geophys. Res. Lett.*, 30 (6), 1318.

Boubnov, B.M. and Golitsyn, G.S. (1995), "*Convection in Rotating Fluids*", Kluwer Academic Publishers, Dordrecht.

Callendar, W., Klymak, J.M. and Foreman, M.G.G. (2011), "Tidal generation of large sub-mesoscale eddy dipoles", *Ocean Sci.*, 7 (4): 487-502.

DiGiacomo, P.M. and Holt, B. (2001), "Satellite observations of small coastal ocean eddies in the Southern California Bight", *J. Geophys. Res.*, 106 (C10), 22,521–22,543, doi:10.1029/2000JC000728.

Dokken, S.T. and Wahl, T. (1996), "Observations of spiral eddies along the Norwegian Coast in ERS SAR images", *FFI Rapport 96/01463*.

Eldevik, T., and Dysthe, K.B. (2002), "Spiral eddies", *J. Phys. Oceanogr.*, 32 (3), 851-869.

Espedal, H.A., Johannessen, O.M., Johannessen, J.A., Dano, E., Lyzenga, D. and Knulst, J.C. (1998), "COASTWATCH'95: A tandem ERS-1/2 SAR detection experiment of natural film on the ocean surface", *J. Geophys. Res.*, 103, 24969-24982.

Font, J., Rousseau, S., Shirasago, B., García-Górriz, E. and Haney, R.L. (2002), "Mesoscale variability in the Alboran Sea: Synthetic aperture radar imaging of frontal eddies", *J. Geophys. Res.*, 107 (C6), 3059, doi:10.1029/2001JC000835.

Gade, M., Byfield, V., Ermakov, S.A., Lavrova, O.Yu. and Mitnik, L.M. (2013), "Slicks as indicators for marine processes", *Oceanography*, submitted.

Golitsyn, G.S. (2012), "On the nature of spiral eddies on the surface of seas and oceans", *Izv. Atmos. Ocean. Phys.*, 48 (3): 350-354.

Karimova, S. (2011), "Eddy statistics for the Black Sea by visible and infrared remote sensing", In: Tang, D. (Ed.), *Remote Sensing of the Changing Oceans*, Springer-Verlag, Berlin Heidelberg, 61-76.

Karimova, S. (2012), "Spiral eddies in the Baltic, Black and Caspian seas as seen by satellite radar data", *Adv. Space. Res.*, 50 (8): 1107-1124.

Lapeyre, G. and Klein, P. (2006), "Impact of the small-scale elongated filaments on the oceanic vertical pump", *J. Mar. Res.*, 64 (6): 835-85.

Marmorino, G.O., Holt, B., Molemaker, M.J., DiGiacomo, P.M. and Sletten, M.A. (2010), "Airborne synthetic aperture radar observations of "spiral eddy" slick patterns in the Southern California Bight", *J. Geophys. Res.*, 115, C05010, doi: 10.1029/2009JC005863.

Munk, W., Armi, L., Fischer, K. and Zachariasen, F. (2000), "Spirals on the sea", *Proc. R. Soc. Lond*., 456, 1217-1280.

Oguz, T., La Violette, P. and Unluata, U. (1992), "Upper layer circulation of the southern Black Sea: its variability as inferred from hydrographic and satellite observations", *J. Geophys. Res.*, 97, 12,569– 12,584.

Robinson, A.R., Golnaraghi, M., Leslie, W.G., Artegiani, A., Hecht, A., Lazzoni, E., Michelato, A., Sansone, E., Theocharis, A. and Unluata, U. (1991), "The Eastern Mediterranean general circulation: features, structure and variability", *Dyn. Atm. Oceans*, 15: 215-240.

Shen, C.Y. and Evans, T.E. (2002), "Inertial instability and sea spirals", *Geophys. Res. Lett.*, 29 (23), 2124, doi: 10.1029/2002GL015701.

Taupier-Letage, I. (2008), "On the use of thermal infrared images for circulation studies: applications to the eastern Mediterranean basin", In: Barale, V. and Gade, M. (Eds.), *Remote Sensing of the European Seas*, Springer Verlag, 153-164.

Titov, V.B. and Savin, M.T. (2008), "Spatial structure of the Black Sea current field", *Meteorol. Gidrol.*, 5, 325-334.

Voropayev, S.I. and Afanasyev, Ya.D. (1992), "Two-dimensional vortex dipoles interactions in a stratified fluid", *J. Fluid Mech.*, 236, 665-689.

Zatsepin, A., Ginzburg, A., Kostianoy, A., Kremenetskiy, V., Krivosheya, V., Stanichny, S. and Poulain, P.-M. (2003), "Observations of Black Sea mesoscale eddies and associated horizontal mixing", *J. Geophys. Res.*, 108 (C8), 3246, doi:10.1029/2002JC001390.

Keywords

Submesoscale eddies, spiral eddies, eddy activity, SAR imagery, Envisat ASAR, surfactant films, wave/current interactions, Black Sea, Mediterranean Sea, Levantine Basin.